RSC Advances

ROYAL SOCIETY OF CHEMISTRY

www.rsc.org/advances

ARTICLE TYPE www.rsc.org/xxxxxx | XXXXXXXX

Atomic structure of icosahedral quasicrystals: Stacking multiple quasi-unit cells

Alexey E. Madison*[a,b]

Received (in XXX, XXX) Xth XXXXXXXXX 200X, Accepted Xth XXXXXXXXX 200X
First published on the web Xth XXXXXXXXX 200X
DOI: 10.1039/b00000000x

An effective tiling approach is proposed for the structural description of icosahedral quasicrystals based on the original substitution algorithm. The atomic structure of icosahedral quasicrystals may by derived by using the iterative and recursive inflation/deflation procedure with subsequent decoration of quasi-unit cells. The quasi-unit cells are stacked in three-dimensional space face-to-face without any gaps between them producing the whole infinite icosahedral structure in the same manner as the usual periodic crystals are generated by multiplication of their unit cells containing one or more atoms in a specific spatial arrangement. A variety of examples illustrating the efficiency of the general algorithm is presented. Stacking of quasi-unit cells along the five-fold axis, as well as the arrangement of cells normal to the five-fold, three-fold, and two-fold axes are presented. The possible atomic structure of an icosahedral single-component quasicrystal is derived. Three types of inequivalent sites with exact icosahedral symmetry may simultaneously exist in the quasicrystalline structure. The structure of characteristic clusters enforced by the compatibility with the quasicrystalline type of ordering is discussed.

Introduction

The discovery of quasicrystals by Shechtman *et al.*[1] revealed new principles for packing of atoms and molecules in solids. Steinhardt *et al.*[2-4] coined the notion of *quasicrystal* and offered the first theoretical explanation of aperiodic crystals. Mackay[5] demonstrated that the diffraction pattern from the Penrose tiling showed all the special features of those from usual crystals lacking only the periodicity. The discovery of quasicrystals and pioneering works on their explanation are now reckoned among the milestones in crystallography.

Significant progress has been achieved in understanding the general principles underlying the structure and behavior of quasicrystals since then,[6-16] but they remained a puzzle in many aspects. Moreover, there is still no generally accepted definition of a quasicrystal.[12] The discreteness of the Fourier transform is adopted as a basis for the new most general definition of an aperiodic crystal.[17,18] However, the self-evident question[19] forces itself upon us – What kinds of order are necessary and sufficient for a pattern of points to have a diffraction pattern with bright spots?

Next question is: Where are the atoms? In general this question is still not fully answered in spite of a great variety of specific structures, which have been explicitly described.[20,21] There are two principal ways of describing the structure of quasicrystals. First of them is based on the higher-dimensional approach[22-24] and uses either the strip-projection of the Ammann grid or the embedding method. The quasiperiodic 3D structure is envisioned as the proper irrational section of a periodic nD crystalline hyperlattice, so that it enables the direct indexing of the experimental diffraction pattern in the nD reciprocal hyperspace.

Higher-dimensional approach is not without shortcomings. It is based on the assumption of a straight strip subjected to the projection from hyperspace. Denial of this assumption leads to stacking faults like phason shifts and to a lot of uncertainties. On the other hand, Steurer and Deloudi[24] showed that the optimum cluster packing in real space may be reached only if the strip follows the boundaries of the interlinked unit cells in the hyperspace, so that the average slope of resulting zigzag lines remains without changes. Therefore, the initial cut-and-project method usually provides the averaged structure information only.[25] In order to derive the true structure from the averaged one, one should have in availability the corresponding electron microscopic images as well as the energetically reasonable configurations of covering clusters. That is why "the powerful but arcane description of quasiperiodic structures as projections from hyperspace has still an aura of mystery" for many researchers.[24]

The second way provides the description of the full quasiperiodic structure by partially overlapping covering clusters.[26-30] The structural similarities between quasicrystals and their rational crystalline approximants facilitate the correct determination of the cluster geometry.[31-37] Another closely related approach is based on the concept of aperiodic tilings and is similar to the description of periodic structures by multiplication of unit cells decorated with atoms.[38] The

[a] *Admiral Makarov State University of Maritime and Inland Shipping, ul. Dvinskaya 5/7, 198035 Saint-Petersburg, Russia. E-mail: alex_madison@mail.ru*
[b] *Center for Advanced Studies, Peter the Great Saint-Petersburg Polytechnic University, ul. Polytechnicheskaya 29, 195251 Saint-Petersburg, Russia*

canonical Danzer tiling[39] is often used for the description of specific icosahedral quasicrystals.[40,41] Both the Danzer tiling and the Socolar-Steinhardt tiling have been shown to be equivalent.[42] Unfortunately, the original deflation rules for the Socolar-Steinhardt tiling cannot be applied iteratively because they do not meet the composition/decomposition requirements.[43] The Danzer tiling is free from this limitation, but very complicated deflation rules and low symmetry of tetrahedral units prevent one from seeing the symmetry of the tiling as a whole and hinder the accurate analysis.

The most recent studies use the combined complex of various methods and approaches.[44,45] However, some important questions remain without clear answers. How to predict the characteristic clusters, if the corresponding crystalline approximant does not exist? How to determine the exact positions of so-called glue atoms? Why do the incomplete or partially fragmented clusters exist? What is the role of such defective clusters?

Engel *et al.*[46] showed that icosahedral quasicrystals can be assembled from a one-component system of particles by means of molecular dynamics simulations. The internal parts of simulated self-assembled particles revealed ordered spatial regions with typical icosahedral clusters. Calculated diffraction patterns along five-fold, three-fold and two-fold axes exhibited sharp Bragg peaks and confirmed the icosahedricity. However, no structures with exact global icosahedral symmetry appeared as a result of simulation. Recently, de Boissieu[47] emphasized that computer simulations of one-component three-dimensional icosahedral quasicrystals will help to understand the mechanisms that may stabilize them in experiments. Surprisingly, no structural models were proposed up to now for an infinite single-component icosahedral quasicrystal.

We are going to offer a solution of this problem.

Recently, we have proposed an effective tiling approach based on the original substitution algorithm.[48] We considered four types of golden zonohedra which form a basic set of tiles for the Socolar-Steinhardt tiling. Next, we adopted the main ideas of the fractal approach[49] bearing in mind that every tile may be fragmented infinitely many times.[50-52] This formalism allowed us to formulate the mutually consistent inflation/deflation rules and natural matching rules for all four types of golden zonohedra. Finally, we have shown how to generate infinite icosahedral tiling from an arbitrarily chosen finite quasicrystalline fragment.[52] All that was lacking in order to make possible the generation of the strongly-regular infinite icosahedral packing of atoms, was the appropriate decoration procedure for zonohedra.

Usual periodic crystals are characterized by their unit cells containing one or more atoms in a specific spatial arrangement. The unit cells are stacked in three-dimensional space face-to-face without any gaps between them. In the same manner, the atomic structure of icosahedral quasicrystals may by derived by using the iterative and recursive inflation/deflation procedure with subsequent decoration of quasi-unit cells. The golden zonohedra properly decorated by atoms may also be stacked in three-dimensional space face-to-face and, also, without any gaps between them so that they produce the infinite consistent packing of atoms with ideal icosahedral order. In comparison with crystals, quasicrystals represent simply another type of ordering and nothing more. The only difference is that the number of unit cells is four instead of single one for usual periodic crystals.

In the present paper, we discuss the details of our substitution algorithm combined with decoration and apply it to icosahedral quasicrystals in order to construct the five-fold, three-fold, and two-fold surfaces. As an example, we demonstrate how to derive the ideal infinite structure of an icosahedral single-component quasicrystal.

Inflation/deflation + decoration

Inflation/deflation rules combined with one of the simplest ways of possible decorations are depicted in the Fig. 1. Before we start the explanation, we would like to quote three very important claims from the paper by Socolar and Steinhardt:[4]

1. "Four types of unit cells appear; the triacontahedron, the icosahedron, the dodecahedron, and the prolate rhombohedron, with volumes in the ratios $10\tau:5\tau:2\tau:1$.
2. There are three complete packings with a (single) center of icosahedral point symmetry. One of these has a triacontahedron at its center, the next shell being composed of thirty dodecahedra. The other two have a star at their centers, one having twelve icosahedra as the next shell, the other having twelve triacontahedra.
3. There is a homogeneity about the packings reminiscent of the Penrose tilings. Given any finite region, there are others identical to it relatively close by."

Combining second and third claims together, we come to conclusion that, in any icosahedral quasicrystal, there always exist exactly three types of sites with icosahedral local symmetry and exactly three different kinds of icosahedral atomic clusters may be always found in the whole packing, no matter whatever a specific structure is under consideration.

Continue with the explanation of the inflation/deflation rules.[48] The four types of unit cells (Fig. 1*i*) are inflated by a factor of τ^3 (Fig. 1*ii*), where τ is the golden mean, and deflated again to the tiles of the original size (Fig. 1*iii*). When the whole tiling becomes generated after performing subsequent iterations of the inflation/deflation procedure, the cells should be decorated by some specific decoration method (Fig. 1*iv*).

When we bear in mind that every cell may be deflated infinitely many times up to the fractal dust, there exist only two types of inequivalent vertices in the whole tiling. We have denoted them as A and B-types, respectively. The A-type vertex corresponds to the center of the star of rhombohedra surrounded by twelve rhombic icosahedra in the next shell, whereas the B-type vertex corresponds to the star of rhombohedra surrounded by twelve triacontahedra. For example, the A-type vertices of the triacontahedron lie on its five-fold axes, whereas the B-type vertices lie on its three-fold axes. We emphasize that both types of vertices have complete icosahedral symmetry in the corresponding fractal parent and that any arbitrarily chosen vertex converges to one of these two types after sufficient iterations of subsequent deflations and inflations.

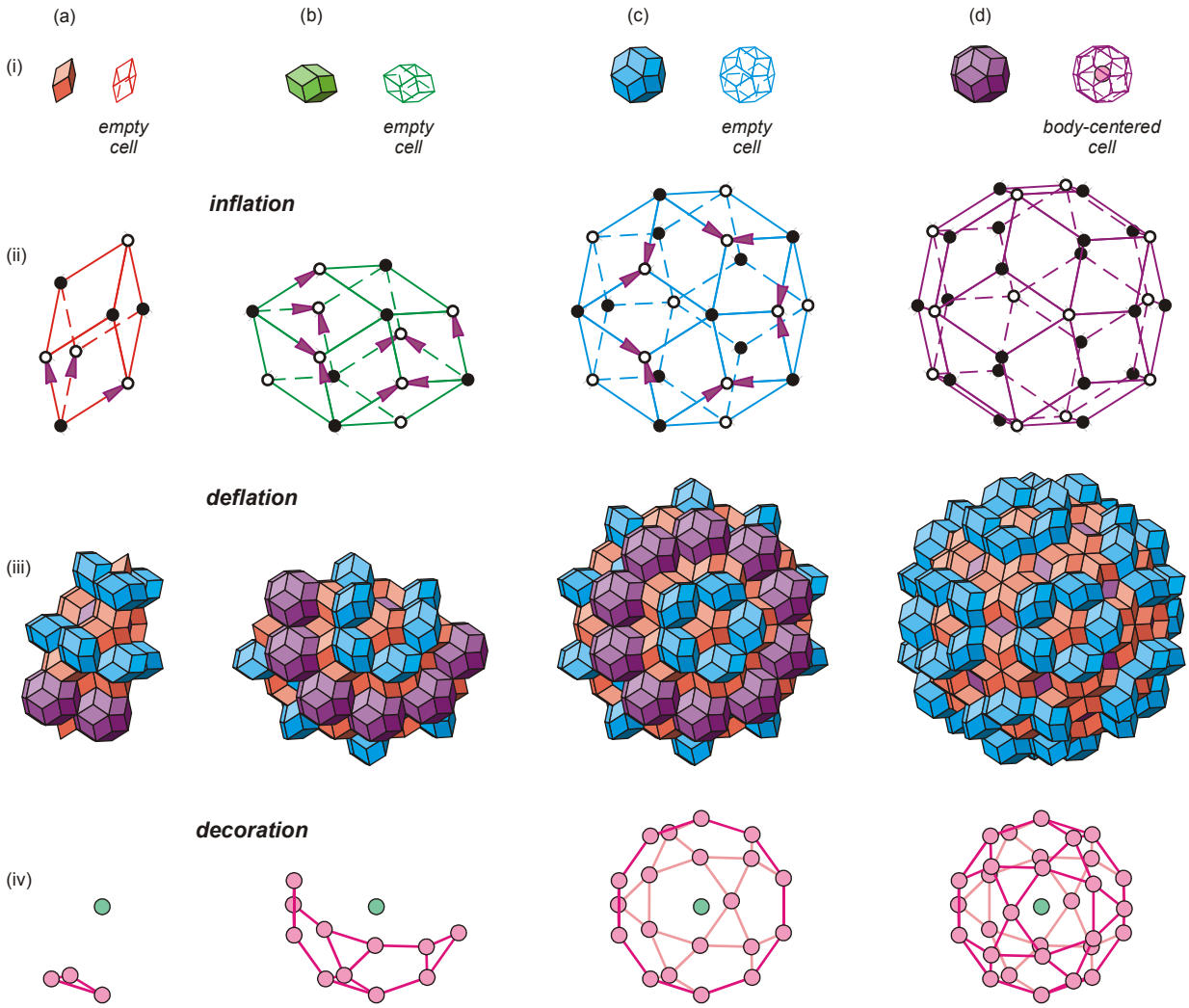

Fig. 1 Inflation/deflation + decoration. (a), (b), (c) and (d) Quasi-unit cells – prolate rhombohedron, rhombic dodecahedron, rhombic icosahedron, and rhombic triacontahedron, respectively. (*i*), (*ii*), (*iii*) and (*iv*) Initial, inflated, deflated, and decorated cells, respectively.

We have also to introduce the C-type site at the center of a triacontahedron surrounded by thirty rhombic dodecahedra. The sites of the last type are not present amongst vertices of the Socolar-Steinhardt tiling because they represent the centers of corresponding cells. In the icosahedral quasicrystal, aforementioned three types of sites represent points with the highest possible local symmetry.

In the whole tiling, there are no edges connecting equivalent vertices, but only the vertices of two alternative types, A and B, may be connected by edges. There are exactly two types of edges. The first type edge E_1, after deflation, will contain a rhombic icosahedron in its middle. The second type edge E_2 will contain a rhombic triacontahedron next to the A-type vertex. We have marked the second type edge by an arrow directed to the A-type vertex, indicating the position of the reduced triacontahedron after deflation.

There are exactly three types of inequivalent faces, namely F_1 (no edges with arrows present), F_2 (two arrows point to opposite A-type vertices), and F_3 (two arrows point to the same A-type vertex).

Natural matching rules[48] ensure that the inflation/deflation procedure may be applied iteratively, so that we can eventually cover the entire space with zonohedra. Moreover, they guarantee that the first type faces of any zonohedron meet only the first type faces of the adjacent cells, the second type faces meet only the second type, and the third type faces meet only the third type, respectively. As a result, the golden zonohedra may be stacked in three-dimensional space face-to-face without any gaps between them. Common edges are shared by the adjacent cells so that no conflicts arise due to existence of two inequivalent types of edges.

In the study of substitutions, from one-dimensional symbolic substitutions to very general tiling substitutions, the substitution matrix is an indispensable tool (see, *e.g.*, the review by Frank[53]). The substitution matrix M is a matrix with entries M_{ij} given by the number of tiles of type i in the substitution of the inflated tile of type j. We refer the reader to the literature for more details.[53-57] It is commonly adopted that

distinct tiles have non-intersecting interiors for the most interesting cases, so that the substitution matrix is always an integer matrix with non-negative entries and the Perron–Frobenius theory is thus relevant.

It is not so in our case. As usually, the substitution matrix is a 4×4 square matrix, which entries correspond to the four types of zonohedra. The tiles are still inflated and then covered by tiles from the original scale, but some of these may partially stick out of the inflated tiles.

Particularly, suppose that the initial volume of the rhombohedron is equal to one.[3,4] If the cell is enlarged with a linear scale factor of τ^3, its volume increases by a factor of $\tau^9=21+34\tau$. The τ^3 times enlarged rhombohedron contains one whole triacontahedron inside and three additional triacontahedra on the edges. These are shared by adjacent cells, so that only one fifth of every triacontahedron belongs to the inflated rhombohedron. Next, there are three rhombic icosahedra, every of which belongs to the inflated cell by as much as one fifth, and six rhombic icosahedra, every of which belongs to the inflated cell by as much as two fifths. Further, three rhombic dodecahedra may be found inside the cell as a whole. Finally, twelve whole and eighteen shared rhombohedra exist in the decomposition. The deflation rules my be analyzed for all four types of zonohedra in a similar way[52] resulting in the following expression:

$$\tau^9\cdot\begin{pmatrix}1\\2\tau\\5\tau\\10\tau\end{pmatrix}=\begin{pmatrix}21+34\tau\\68+110\tau\\170+275\tau\\340+550\tau\end{pmatrix}=\begin{pmatrix}21 & 3 & 2\frac{2}{5} & 1\frac{3}{5}\\ 68 & 11 & 6\frac{2}{5} & 5\frac{3}{5}\\ 170 & 20 & 17 & 15\\ 340 & 30 & 36 & 31\end{pmatrix}\cdot\begin{pmatrix}1\\2\tau\\5\tau\\10\tau\end{pmatrix} \quad (1)$$

Here, the entries of the column matrices represent the relative volumes of zonohedra – initial and τ^3 times enlarged ones, respectively. The transpose of a matrix in the right part of this equation is the desired substitution matrix. Note that some entries are not integer. Thus, the substitution rules are so-called "imperfect" in our case.

After the entire space is filled by zonohedra, we can decorate the cells with atoms in a specific spatial arrangement producing the desired atomic structure. The matching rules should cause some additional restrictions due to the interlinkage of different cells, but we cannot yet formulate these restrictions rigorously. The simplest way of possible decoration is obvious. We can suppose that either A, or B, or C-type positions are occupied by specific atoms, whereas all others remain unoccupied. This results in three different examples of single-component icosahedral quasicrystals. Every of them will have specific triad of characteristic clusters, each of which will be repeated hierarchically as the main structural motif in corresponding clusters of clusters.

Specifically, suppose that all quasi-unit cells are empty, except for the triacontahedron which we decorate with a single atom at its center (Fig. 1d,*i*, right). After inflation and deflation, the τ^3 times enlarged triacontahedron will contain a hierarchical cluster in the form of icosidodecahedron built of thirty triacontahedra, plus an additional triacontahedron at its center. Therefore, after a subsequent decoration, the triacontahedron transforms into the body-centered icosidodecahedron. Similarly, the rhombic icosahedron turns into the halved icosidodecahedron, the rhombic dodecahedron turns into the cluster resembling the orange lobule, and the prolate rhombohedron turns into the cluster of four atoms in the form of elongated tetrahedron (Fig. 1*iv*). Note that initial zonohedra represent the basic tiles in a certain mathematical tiling pattern. The clusters derived from them as a result of decoration consist of real atoms and reflect the special features of real atomic packing.

In the same manner as four types of zonohedra cover the entire space face-to-face, four types of atomic clusters, being interlinked, cover the same space resulting in an infinite icosahedral quasi-lattice. Generated by this method, atomic positions may by occupied by one single component. Thus, such decoration represents one of possible solutions of the problem raised by de Boissieu.[47] We have to emphasize again that the triacontahedron centering is not the only possible way of decoration.

Self-similar rods

The main concept based on the packing of decorated zonohedra within the τ^3-inflated supercells is not new. Yamamoto *et al.*[58] investigated the structure of *i*-Al-Pd-Mn quasicrystals within a six-dimensional cluster model. They pointed out that earlier works on the structure determination, based on simple large occupation domains and atomic surfaces placed at high symmetry points in a higher-dimensional space, can explain the intensity of strong reflections only, but such approaches are not sufficient to describe the detailed quasicrystal structures. We would like to give a direct quotation – "The use of complicated subdivisions is not avoidable for a detailed structure refinement of quasicrystals." So, they proposed to introduce the atom shift from the ideal positions. As a result, the probable stacking order along the high-symmetry directions was offered and the possible decoration of triacontahedra and stars of rhombohedra by specific atoms was derived. Unfortunately, only three types of quasi-unit cells, instead of four, were involved in the tiling, the possible asymmetry of quasi-unit cells was not taken into account, and some of triacontahedra were allowed to overlap. As a consequence, the Yamamoto-Takakura-Tsai model[53] was not consistent with the Socolar-Steinhardt tiling,[4] and the iterative application of the proposed rules was not possible. Moreover, it was not even assumed. Recall the widely accepted point of view that quasicrystals cannot be defined as packing of identical unit cells, and that their ideal state may be described as a unique way of packing by *overlapping* clusters only.[30] This may be caused by mixing up the terms of "identical copies of a single unit cell" and "identical copies of multiple unit cells from a given set".

In contrast, our substitution algorithm[48] is fully consistent with the Socolar-Steinhardt tiling.[4] Since we remain within the frameworks of the three-dimensional formalism, the structure details become much more evident. Thus, our first goal is to describe some special features of the Socolar-Steinhardt tiling which escaped the attention of researchers for about thirty years.

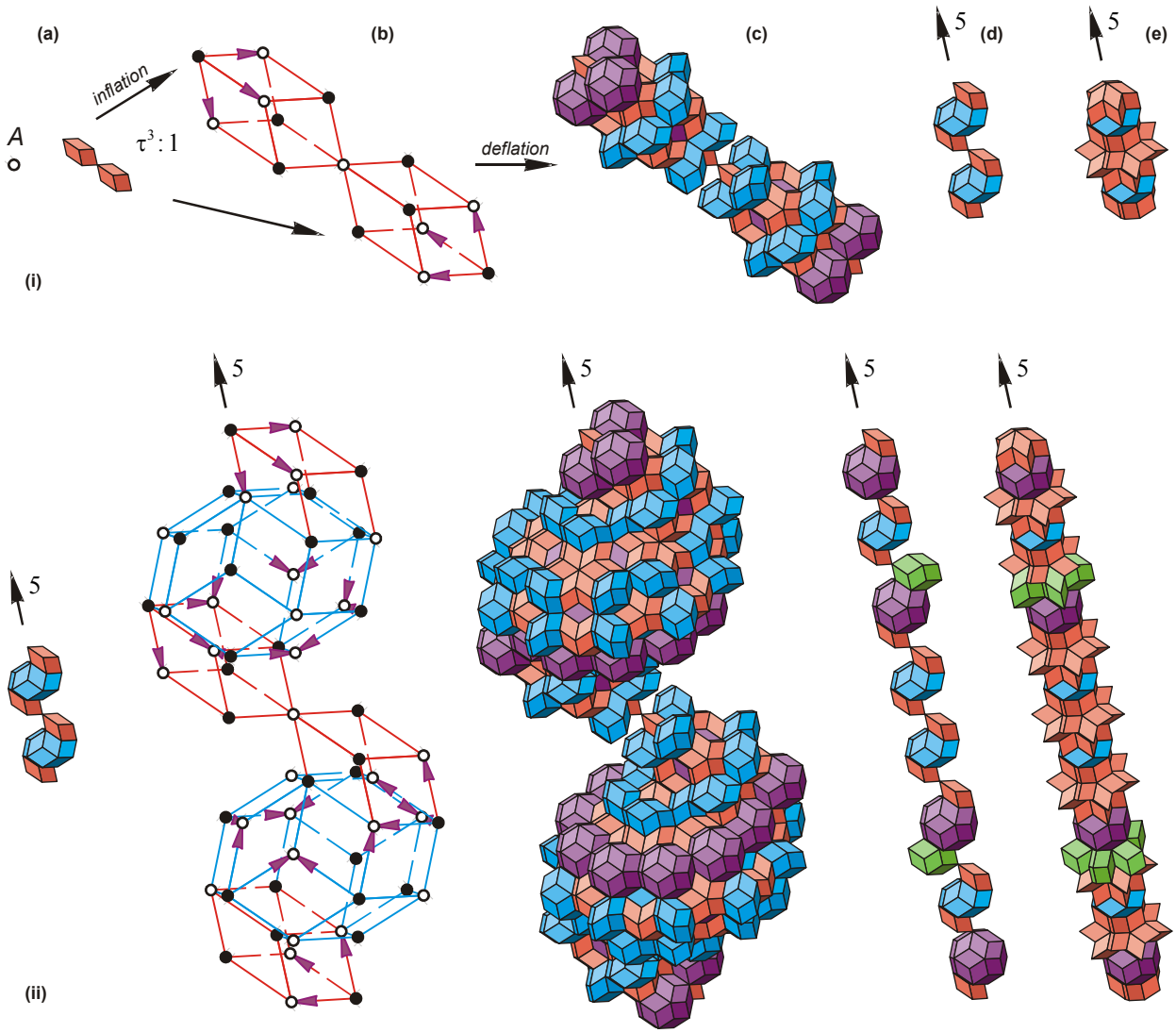

Fig. 2 Generation of self-similar chains. Stacking quasi-unit cells along the 5-fold axis around the A-type site. (a) Initial local environment of the A-type site. (b), (c) Inflation and deflation, respectively. (d) Picking out the cells stacked along the 5-fold axis. (e) Final stacking sequence. (*i*) and (*ii*) 1st and 2nd iterations, respectively. New cells appear next to the just generated ones at each subsequent iteration.

As an example, we now derive the characteristic packing sequences along the symmetry axes in an ideal icosahedral quasicrystal. Consider stacking of cells along the five-fold direction.

Choose an arbitrary A-type site as a starting point and perform a pair of operations, deflation with subsequent inflation, two times in a row according to the rules described above. A local environment turns into a star of rhombohedra, no matter which cells surrounded the chosen site before. Next, pick out the rhombohedra stacked along the five-fold axis (see Fig. 2a), inflate them in a ratio of τ^3 (Fig. 2b), and deflate back to the original size (Fig. 2c). Finally, pick out only the cells stacked along the five-fold axis (Fig. 2d) and rotate them around the symmetry axis (Fig. 2e). As a result of the first iteration (Fig. 2*i*), we have got the order of cell sequence in the same direction, but in an enlarged scale. The position of the initial A-type site remained without changes, as well as those of both nearest-neighboring rhombohedra, but now new cells arose right next to them. Further, we can perform the second iteration (Fig. 2*ii*) and define the next neighboring cells. New cells appear next to the just generated ones at each subsequent iteration. Adding new cells causes no permutations within the already generated segments.

Let's assume, for specificity's sake, that the edges of quasi-unit cells have the unit length. The first iteration applied to the local environment of the point A moves the image of the nearest-neighboring point B to the new position at the distance of $\tau^3=1+2\tau$ from the origin. The second iteration creates another image of the initial point B at the distance of $\tau^6=5+8\tau$, as well as new images of all newly generated points. The third iteration will create the image at the distance of $\tau^9=21+34\tau$, and so forth. As a result, the quasi-unit cells become strongly ordered along the five-fold symmetry axis of an icosahedral quasicrystal and form a highly symmetrical self-similar rod. More detailed description of this procedure may be found elsewhere.[52]

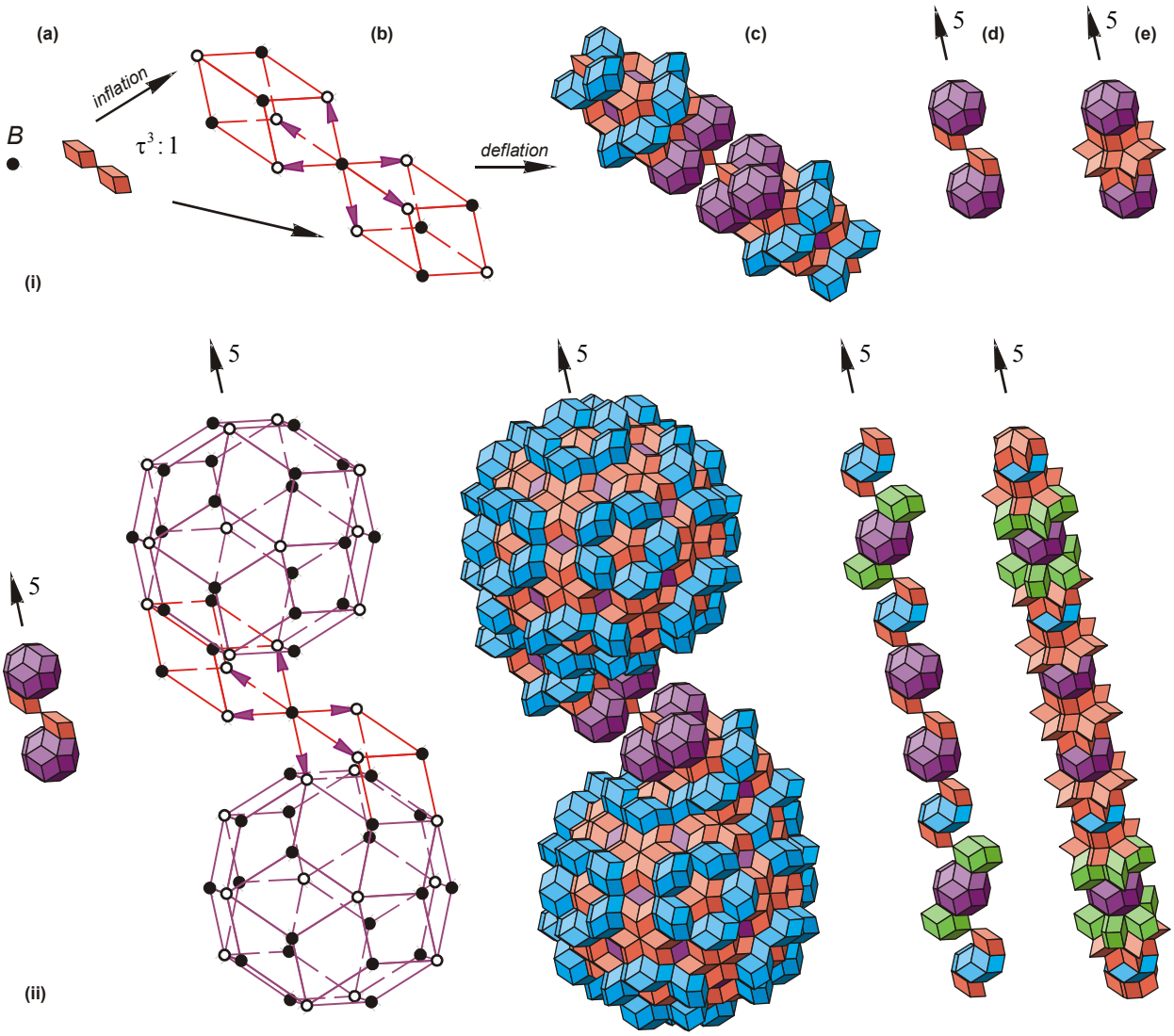

Fig. 3 Generation of self-similar chains. Stacking quasi-unit cells along the 5-fold axis around the B-type site. (a) Initial local environment of the B-type site. (b), (c) Inflation and deflation, respectively. (d) Picking out the cells stacked along the 5-fold axis. (e) Final stacking sequence. (*i*) and (*ii*) 1st and 2nd iterations, respectively. Twenty rhombohedra are arranged into the star around the B-type site in a different way and thus produce another sequence.

Choose an arbitrary B-type site and repeat the above steps. As previously, we start with the star of twenty rhombohedra, but note again that opposite sides of cells are not equivalent. The same rhombohedra form the same star, but now they are arranged in a different way. Therefore, we get another strongly ordered sequence of quasi-unit cells along the five-fold symmetry axis (Fig. 3). As earlier, the initial environment remains unchanged and every subsequent iteration adds new cells to the initial chain. This process may be continued up to infinity.

When starting with a single triacontahedron, we get the third desired sequence (Fig. 4). All the three self-similar chains – centered at A, B, and C-type sites, respectively – possess the central symmetry.

Let's clarify the claim on the homogeneity of the tiling.[4] For instance, suppose that we have generated all three infinite chains of cells, namely with A, B, and C-sites at their origins. Then, any arbitrarily large but finite sized subsequence randomly cut from one of three chains will appear infinitely many times in any of three infinite chains. Virtually, there exists the only one *fractal* sequence. The further from the origin of the C-type chain we consider specific A or B-type sites, the larger may be their undisturbed local environments, and *vice versa*.

Now we describe the alternating of cells along two- and three-fold axes very briefly. For example, we set the origin at the C-type site and thus start with a triacontahedron. After the first iteration, the position of the central triacontahedron remains without changes but it becomes surrounded by two rhombic dodecahedra and additional two triacontahedra from both sides along the two-fold axis. After the second iteration, every triacontahedron turns into the aforementioned subsequence, whereas the rhombic dodecahedra turn into the chains of dodecahedra surrounded by two triacontahedra. Eventually, we get the chain of alternating subsequences of either one or two triacondahedra spaced by dodecahedra.

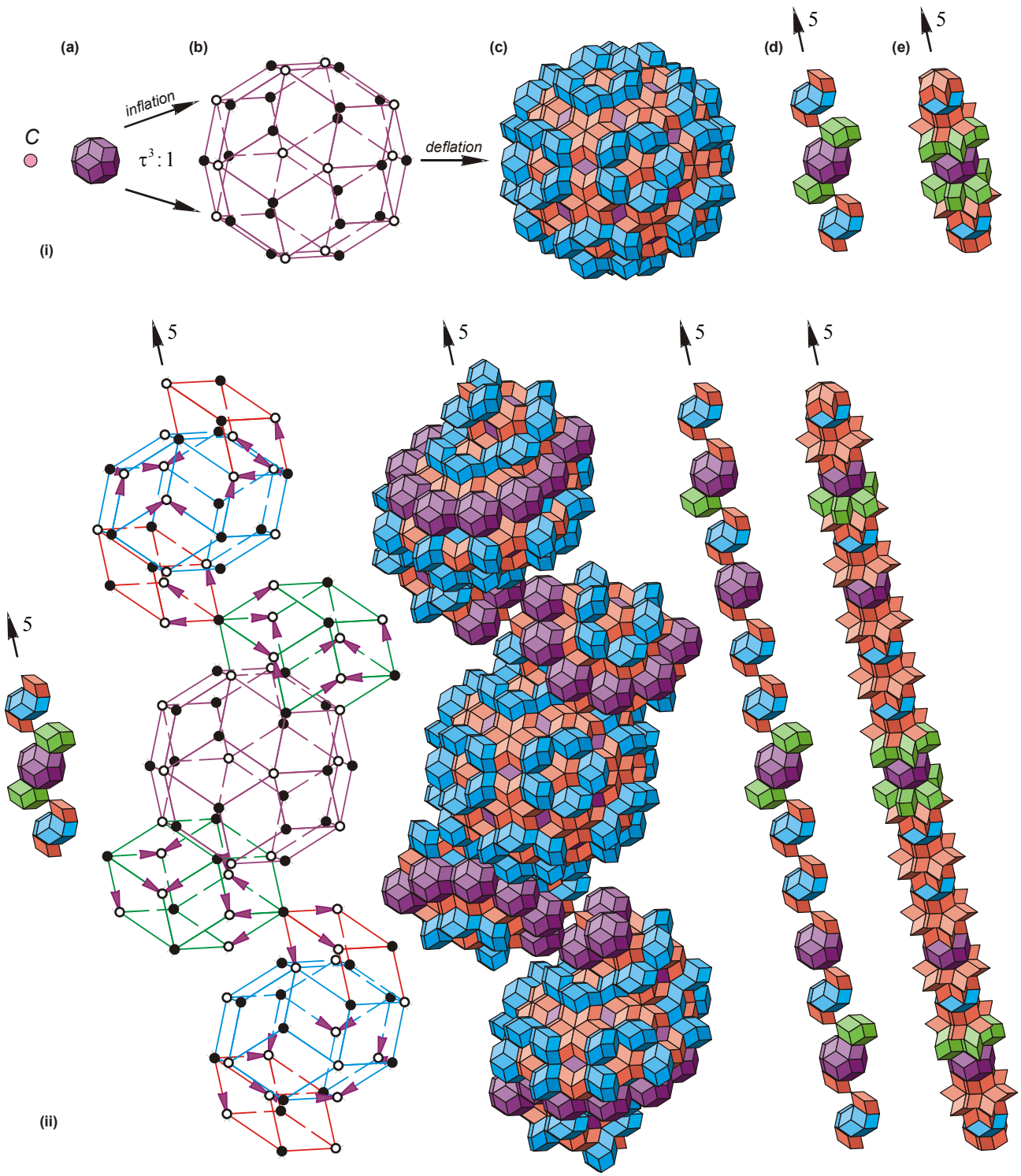

Fig. 4 Generation of self-similar chains. Stacking quasi-unit cells along the 5-fold axis around the C-type site. (a) Initial triacontahedron and initial local environment of the C-type site. (b), (c) Inflation and deflation, respectively. (d) Picking out the cells stacked along the 5-fold axis. (e) Final stacking sequence. (*i*) and (*ii*) 1st and 2nd iterations, respectively.

When considering the stacking of cells along the three-fold axis, we start with the same triacontahedron again. Three-fold axis passes through the B-type vertex. After the first iteration, the central triacontahedron becomes surrounded by two pairs of elongated rhombohedra from both sides along the three-fold axis. The rhombohedra share the common A-type vertices, so that the subsequence terminates with the B-type vertex again. After the second iteration, every triacontahedron

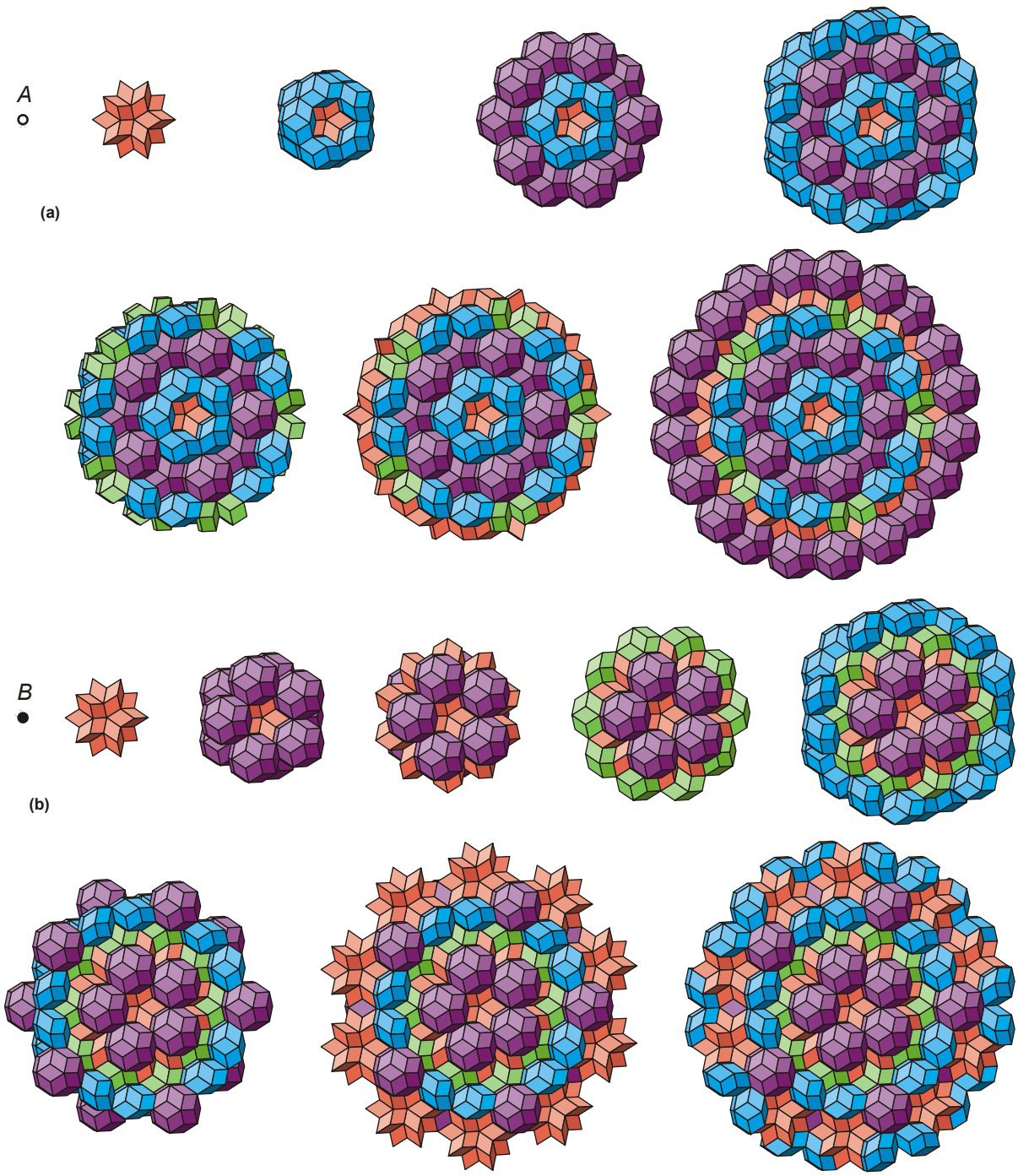

Fig. 5 Generation of self-similar layers perpendicular to the 5-fold axis. (a) and (b) Layers centered at the A and B-type sites, respectively.

turns into the aforementioned subsequence, whereas the each pair of rhombohedra turns into the pair of rhombohedra surrounded by two triacontahedra and by two next pairs of rhombohedra. Eventually, we get the chain of alternating subsequences of either one or two pairs of rhombohedra spaced by single triacondahedra.

Such properties are characteristic of the Fibonacci sequence but, in contrast, our chains are infinite in both directions and possess the central symmetry.

Quasiperiodic surfaces

Quasiperiodic surface order leads to several intriguing features, such as a puzzling resistance to surface oxidation, lower friction, and surprisingly good catalytic activity. Quasicrystals can enforce their bulk order in films, thus opening new perspectives as potential templates. Most of these special features are deeply related to the bulk atomic structure, but the most puzzles are understood only superficially even now. For more comprehensive surveys, we

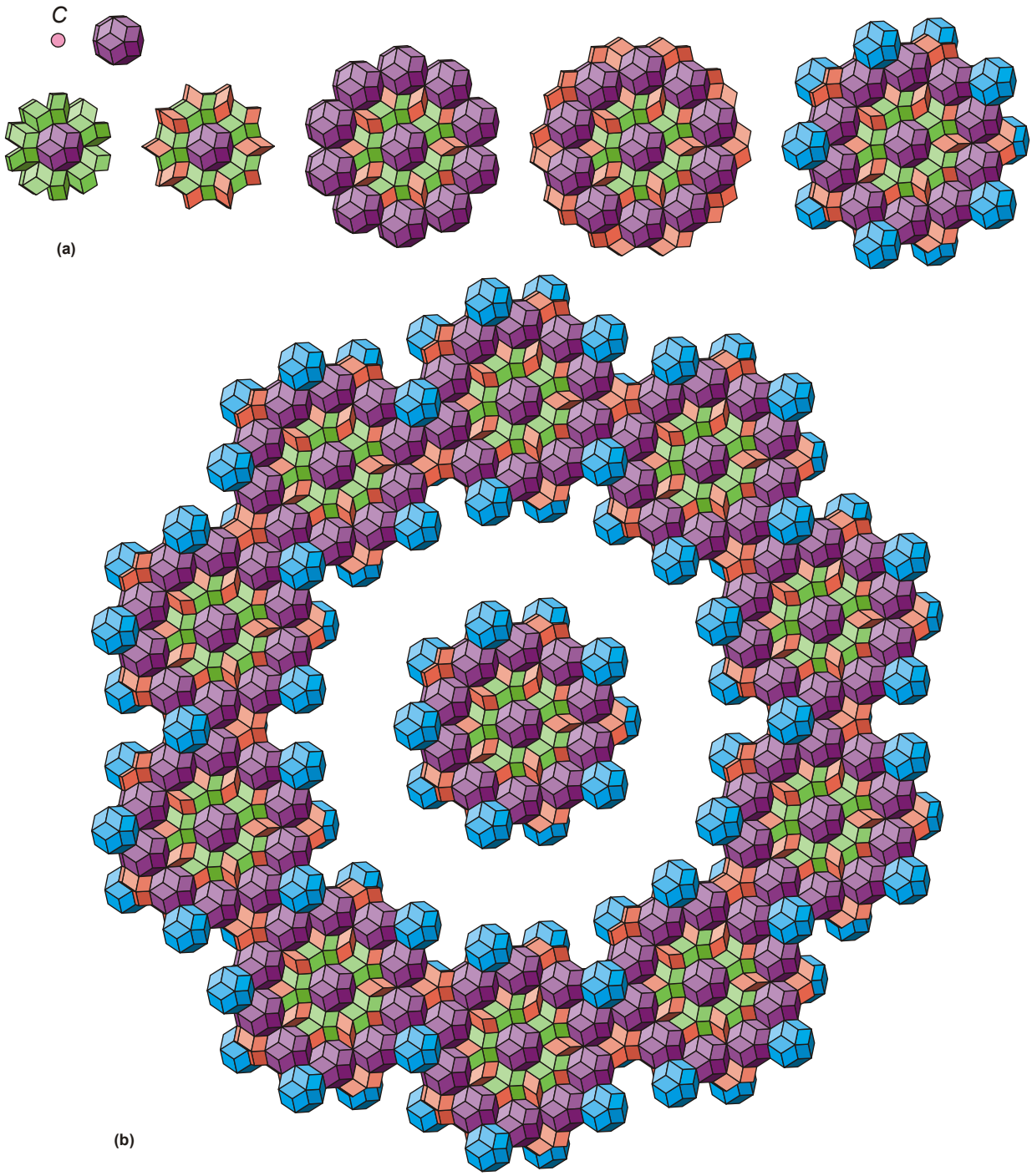

Fig. 6 Generation of the self-similar 5-fold layer centered at the C-type site. (a) The central triacontahedron transforms into the hierarchical cluster containing the ring of triacontahedra. (b) Every of ten triacontahedra moves τ^3 as far from the origin as it was before and turns into the same supercluster.

refer the reader to recent reviews on the surface science of quasicrystals.[59-61]

In our opinion, the plane surface cannot be comprehensively interpreted in terms of the plane tiling. Indeed, the Penrose tiling has two different sites with the local five-fold symmetry. On the contrary, we will demonstrate that three different sites with exact five-fold symmetry can exist on the unreconstructed five-fold surface of an icosahedral quasicrystal. Furthermore, the very successful interpretation of the five-fold surface by means of the Penrose tiling will be of no use when a surface of another orientation becomes the next subject of interest. We will show how the atomic structure of any surface may be derived based on the common assumptions of the fractal approach.

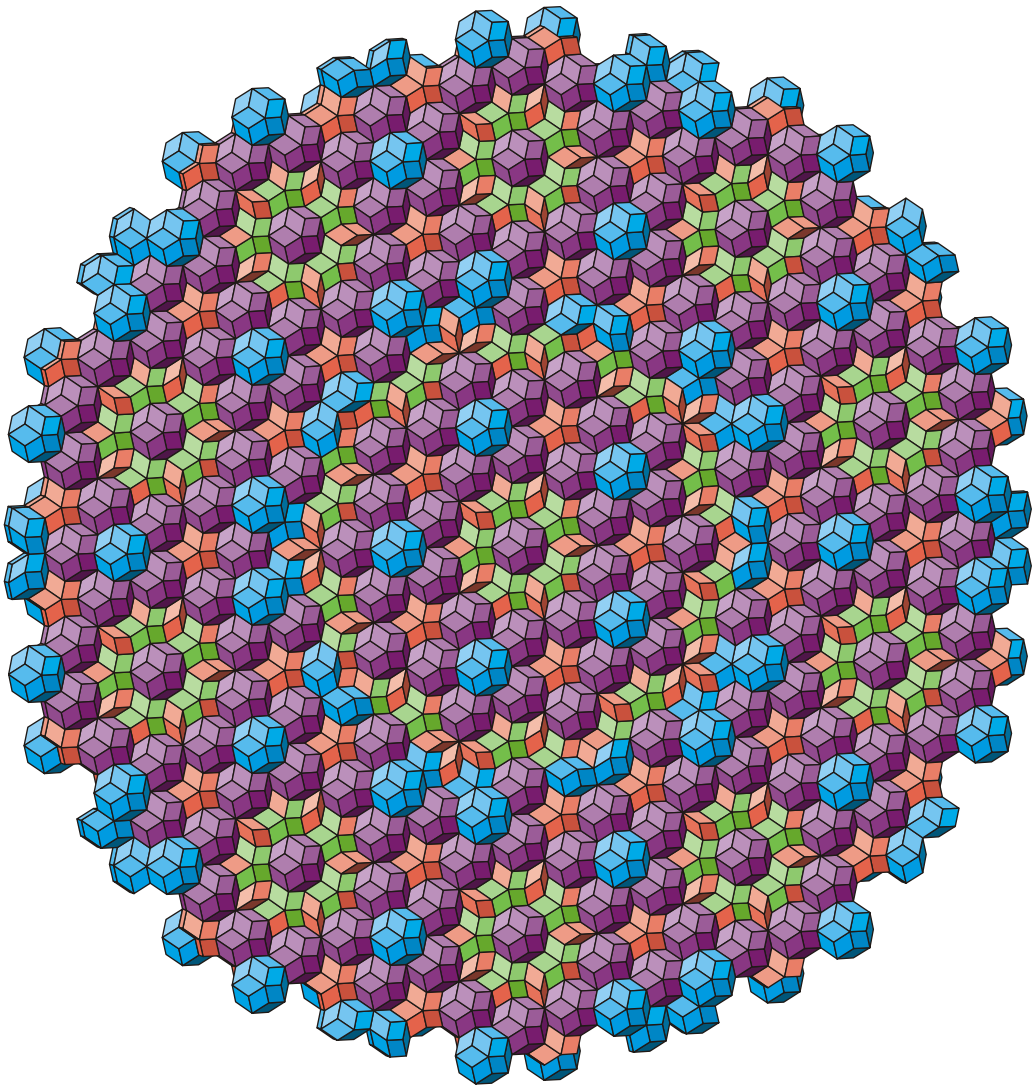

Fig. 7 Self-similar 5-fold layer centered at the C-type site.

In order to derive the models of unreconstructed surfaces, we superpose the origin with the A, B, and C-type sites, respectively, and slice the corresponding layers from the bulk of an infinite icosahedral tiling normal to the symmetry axes. The corresponding five-fold layers derived according to the substitution rules[48] are presented in the Figs. 5-7.

Very characteristic hierarchical clusters of clusters may be detached from the entire infinite packing. When the origin is superposed with the A-type site at the center of the corresponding star, the triacontahedra form two distinct shells around the origin. The inner shell is represented by a Platonic dodecahedron, each vertex of which is occupied by a triacontahedron. The outer shell is an Archimedean solid – the equilateral truncated dodecahedron – with triacontahedra at its vertices. All triacontahedra are closely stacked face-to-face. The shells correspond to rings of triacontahedra on the cross-section (Fig. 5a).

When the origin is superposed with the B-type site, the second characteristic cluster of clusters may be found. Its inner shell is represented by an icosahedron made of triacontahedra stacked face-to-face. The outer shell is a dodecahedron made of more distanced triacontahedra (Fig. 5b).

The most intriguing case is when the origin is superposed with the center of a triacontahedron. Consider the subsequently inflated and deflated triacontahedron (Fig. 1d,*iii*) and slice it normal to the five-fold axis (Fig. 6a). A remarkable cluster appears. It has the very notable structural motif of a ring of ten triacontahedra stacked face-to-face around the central triacontahedron. This plane motif corresponds to a cross-section of an hierarchical cluster of clusters – icosidodecahedron built of triacontahedra.

Now we take a next step and inflate a just obtained cluster according to the same rules. The central triacontahedron transforms once again into the hierarchical cluster which we have seen already. Every of ten ring-shape arranged triacontahedra moves τ^3 as far from the origin as it was before and turns into the same supercluster. Another remarkable

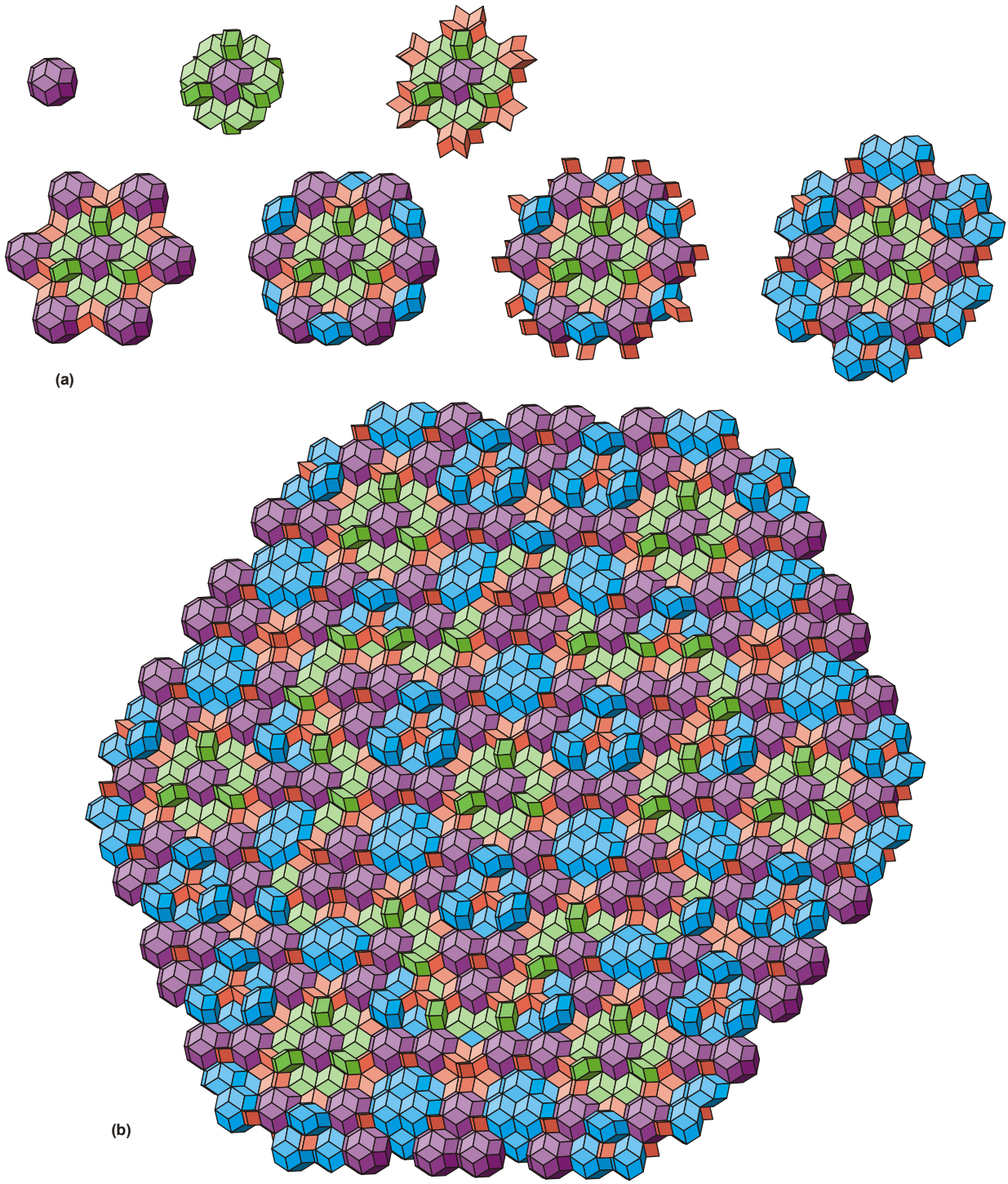

Fig. 8 Self-similar 3-fold layer centered at the C-type site. (a) and (b) 1st and 2nd iterations, respectively.

cluster appears – a hierarchical wheel built of ten rings of ten triacontahedra (Fig. 6b). This wheel, in turn, represents a cross-section of an icosidodecahedron built of icosidodecahedra, each of which is built of triacontahedra. Finally, we fill the interstitial space by inflating and deflating the rhombic dodecahedra in between (Fig 7). Natural matching rules ensure that the adjacent cells fit together after any iteration. This process may be continued up to infinity producing an amazing intricate "chainmail" of interlinked rings of rings of rings ... of rings of triacontahedra.

Compare the central part of the obtained layer (Fig. 7) with the unit cell configurations in the Socolar-Steinhardt tiling (see Fig. 9 in the original paper by Socolar and Steinhardt[4]). The identity becomes evident. The central part of the slice contains the ring of ten triacontahedra stacked face-to-face surrounded by ten interlinked pentagons made of

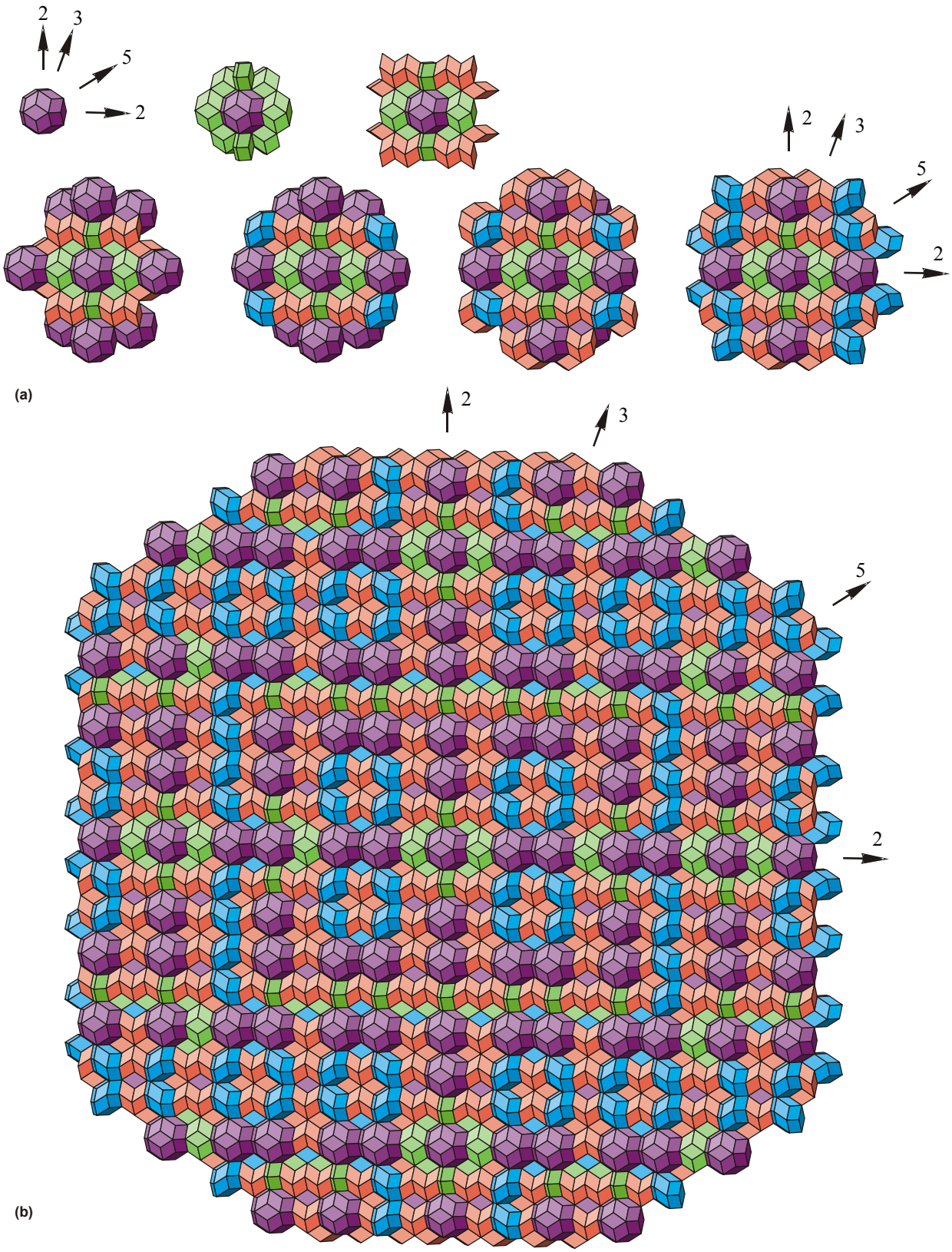

Fig. 9 Self-similar 2-fold layer centered at the C-type site. (a) and (b) 1st and 2nd iterations, respectively.

triacontahedra in the same manner. The substitutions and the Ammann grid projection produce equivalent results!

We can also slice the icosahedral packing by planes normal to the 3rd and 2nd order axes, respectively. The corresponding

three-fold and two-fold layers are presented in the Figs. 8,9. The aforementioned Fibonacci-like alternation of triacontahedra and rhombic dodecahedra along the two-fold axis as well as the alternation of elongated rhombohedra and triacontahedra along the three-fold axis may be seen in the Fig. 9. These chains simultaneously present in the layer sliced normal to the two-fold axis.

We hope that our models will be useful in the surface investigations of actual quasicrystals.[62-68] In particular, the distribution of triacontahedra within the five-fold layers seems to resemble the local configurations on surfaces of icosahedral Al-Pd-Mn quasicrystals[66] – so-called "rings" and "white flowers." When replacing the triacontahedra with dots within the three-fold layers, the as-obtained structural motif resembles the atomic structure of the three-fold surface of the icosahedral Ag–In–Yb quasicrystal,[67] namely the distribution of the Yb atoms, and so on.

Stacking multiple quasi-unit cells

Let's show which kinds of icosahedral atomic clusters arise and how they are interlinked into the whole structure when, for example, the only C-type sites are occupied by single atoms (Fig. 1*iv*). Three complete packings with a single center of icosahedral point symmetry[4] produce three characteristic types of shell clusters in any icosahedral quasicrystalline structure. As a consequence, three types of interlinked multi-shell clusters will simultaneously co-exist in the particular case we are interested in.

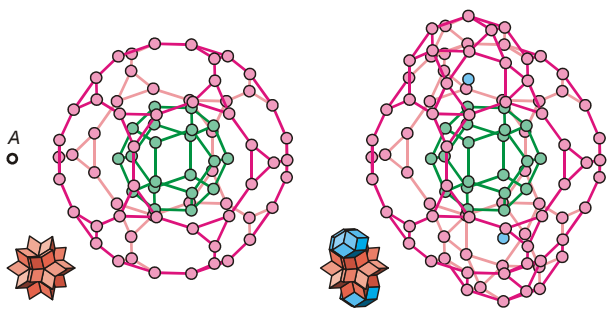

Fig. 10 Characteristic cluster in the structure of a single-component icasahedral quasicrystal centered at the A-type site. Atomic clusters are derived from corresponding clusters of zonohedra.

Consider the local environment of the A-type site. Twenty rhombohedra arranged together around the A-type site form a star. Every rhombohedron turns into an elongated tetrahedron after decoration (Fig. 1a,*iv*). After multiplication, the single detached atom produces a Platonic dodecahedron, whereas the more distant triangle turns into an equilateral truncated dodecahedron (Fig. 10). The second shell of the tiling is formed by twelve rhombic dodecahedra, each of which turns into a halved icosidodecahedron after decoration, so that every ten-fold atomic ring in the previous shell becomes centered and caped. The characteristic cluster of the A-type site surrounded by C-type atoms may be described as follows: $C_{20}@C_{60}@(C_1+C_{10})_{12}$.

The local environment of the B-type site may be considered in the same manner. Twenty rhombohedra arranged together around the B-type site form a star again. But now, the triangles produce the inner icosahedron, whereas the detached atoms produce a larger dodecahedron (Fig. 11). The second shell of the tiling is formed by twelve triacontahedra, each of which turns into a complete icosidodecahedron as a result of decoration, so that the adjacent icosidodecahedral balls appear next to the faces of the large dodecahedron. The characteristic cluster of the B-type site surrounded by C-type atoms may be described as follows: $C_{12}@C_{20}@(C_1@C_{30})_{12}$.

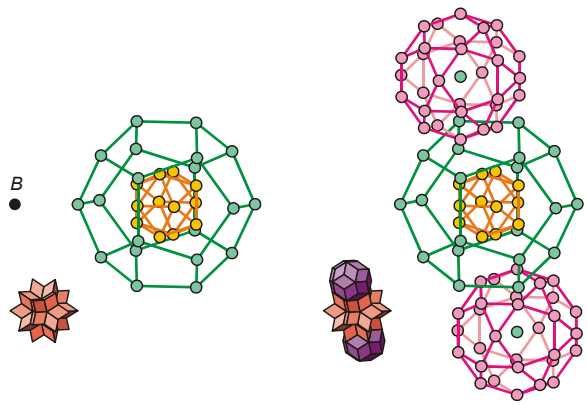

Fig. 11 Characteristic cluster centered at the B-type site. Atomic clusters are derived from corresponding clusters of zonohedra.

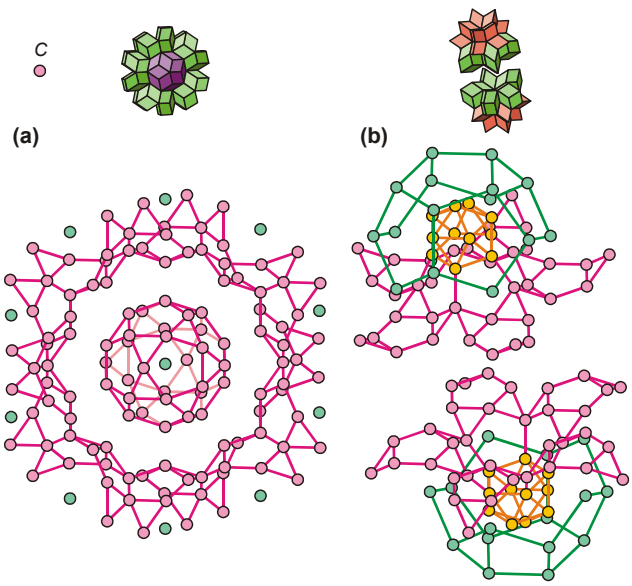

Fig. 12 Characteristic cluster centered at the C-type site. (a), (b) Atomic arrangements in the plane perpendicular to and along the 5-fold axis, respectively. Icosidodecahedron at the center between two "lily flowers" (right) is not shown.

The characteristic cluster of the C-type site surrounded by C-type atoms is already derived (Fig. 1d,*iv*) – $C_1@C_{30}$.

The local environment of the C-type site shows the amazing alternation of the convex and concave atomic surfaces. The

central icosidodecahedron becomes surrounded by interlinked lobules in the five-fold plane (Fig. 12a). The same lobules form lily flowers with five petals in the normal direction, so that every icosidodecahedral ball becomes surrounded by opposite flowers along the five-fold axis (Fig. 12b). The entire hierarchical ring (Fig 7), after complete decoration, turns into the wheel of ten interlinked icosidodecahedra (Fig. 13). The role of glue atoms[69] is clearly seen. The inner ring of ten atoms is surrounded by ten pentagons. Thus, the τ^3 times larger wheel of ten interlinked icosidodecahedra will be surrounded by the ring of ten pentagons with interlinked icosidodecahedra at their vertices (not shown in the Fig. 13), and so forth.

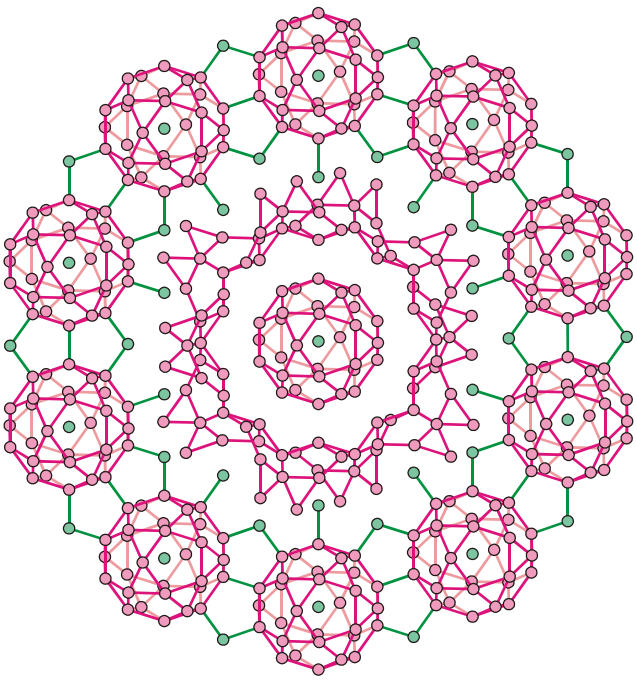

Fig. 13 Hierarchical ring of ten interlinked icosidodecahedra surrounding the C-type site.

Decoration of zonohedra makes it possible to derive the stacking sequences of characteristic clusters along the high-symmetry directions. In particular, the alternating order of characteristic clusters along the 5-fold axis derived from the upper half of the chain centered at the C-type site (Fig. 4e,*ii*) is presented in the Fig. 14. The lowermost icosidodecahedron is the decoration result of the central triacontahedron in the C-type chain of zonohedra. All atomic positions are generated according to the common algorithm from the position of the only atom initially placed at the origin.

Now we can compare our results with one of the most representative examples of icosahedral quasicrystals, namely, with the structure of the stable binary alloy Yb-Cd.[6] We have to highlight two special features. The first one is the inflation factor of τ^3. The inflation factor in our consideration has the same value. Recall that the canonical tiling has the inflation factor of τ. Second, the main structural motif is represented by a very remarkable hierarchical cluster – the τ^3 times inflated supercluster in the form of icosidodecahedron consisting of

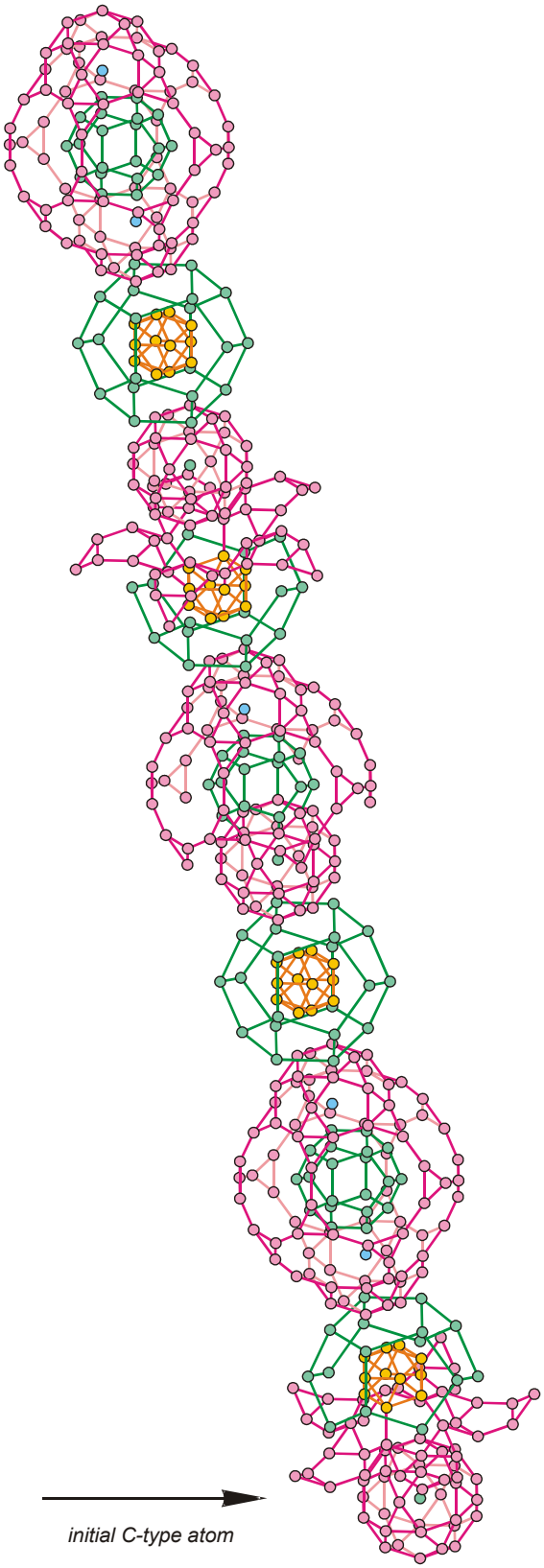

Fig. 14 Stacking sequence of characteristic clusters along the 5-fold axis derived from the upper half of the chain centered at the C-type site. All atoms are generated from the only atom initially placed at the origin.

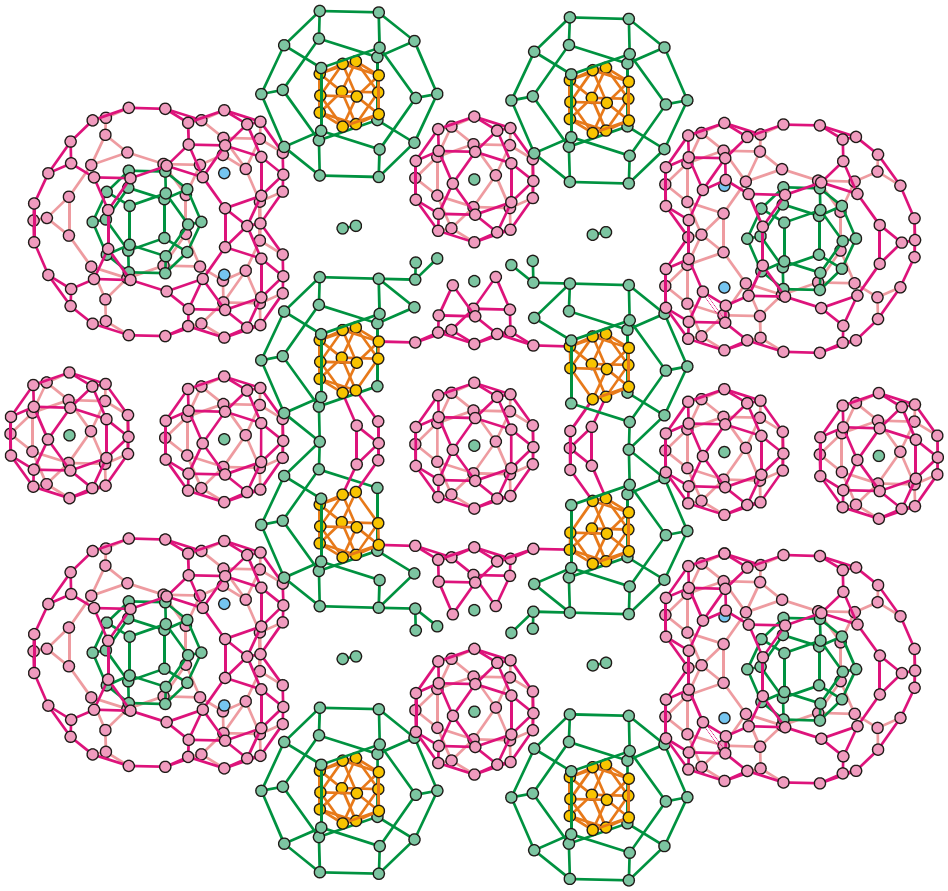

Fig. 15 Atomic structure of a single-component icosahedral quasicrystal in projection on the two-fold plane. All three types of characteristic clusters co-exist simultaneously.

thirty icosidodecahedra formed by Yb atoms. This is in a good agreement with our theoretical results.

On the other hand, the plane that is usually described as being seen along the five-fold axis in the structure of Yb-Cd alloy does not reveal the exact five-fold symmetry (see, *e.g.*, Fig. 5 in the paper by Takakura *et al.*[6]). It is not clear, either this fact is due to uncertainties in the determination of the glue atom positions or due to the influence of the most inner tetrahedral shells of the Tsai clusters that could enforce the symmetry lowering up to the tetrahedral symmetry. In any case, the ideal structure with exact icosahedral symmetry would be of special interest. Our models satisfy this requirement.

The projection on the two-fold plane is the most informative (Fig. 15). All three types of characteristic clusters simultaneously present in this plane after decoration forming a notable triangle Δ ABC – its first vertex coincides with the center of the initial triacontahedron, two others coincide with two alternating vertex types of the τ^6 times enlarged triacontahedron. We emphasize that any packing of atomic clusters presented by us (*e.g.*, Fig. 15) is derived from the corresponding space tiling by zonohedra (Fig. 9b, respectively) by following the common substitution rules and chosen decoration method.

So, if the C-type site is occupied by a single atom, the centered icosidodecahedron becomes the most characteristic pattern that is hierarchically repeated throughout the entire structure. The C-type cite is occupied by the icosidodecahedron itself. Its τ^3 times enlarged local environment is represented by an hierarchical cluster – τ^3 times enlarged icosidodecahedron with each vertex occupied by the icosidodecahedra, and so forth. The local environment of the A-type site is represented by a dodecahedron inside the truncated dodecahedron with centered large faces caped by halved icosidodecahedra. Its τ^3 times enlarged local environment corresponds to the similar cluster, but with every vertex occupied by icosidodecahedra. The local environment of the B-type site is represented by an icosahedron inscribed inside the dodecahedron. Its τ^3 times enlarged local environment corresponds to the similar cluster, but with every vertex occupied by icosidodecahedra, and so forth.

If the A-type site is occupied by an atom, then the centered icosidodecahedron, icosahedron, and larger icosahedron form the most inner shells of characteristic clusters at the A, B, and C-type sites, respectively. If the B-type site is occupied by an atom, then icosahedron, centered icosidodecahedron, and large dodecahedron form the most inner shells of characteristic clusters at the A, B, and C-type sites, respectively. Other

possibilities arise when more general positions at the centers of corresponding edges and faces (E_1, E_2, F_1, F_2, and F_3) are taken into account. We are going to present all clusters compatible with quasicrystalline ordering type, with their relative positions and shell sizes, in a separate paper.

Consider the characteristic clusters in more details. First of all, we have to draw the reader's attention to the fact that the nearest interatomic distance may have three different values (see Fig. 15) – this agrees with the fact that oscillating pair potentials may stabilize the icosahedral structure.[46,47] Various atoms have different local arrangement, although they are all originated from fully equivalent positions by decorating the equivalent zonohedra. The apparent contradiction may be cleared by the following reasoning. We can chose an arbitrary atom with its local environment, recover the description by closely stacked zonohedra, perform the deflation/inflation procedure two times in a row – this affects only the scale of consideration – and redecorate the tiling. The described procedure replaces the local environment of any atom by the standard one with simultaneous rescaling of the structure as a whole. Atomic positions are not equivalent in the conventional sense. On the other hand, when the deflation is performed up to infinity, they are absolutely equivalent in the corresponding fractal parent. Of course, we have to come to a stop somewhere, due to the atomicity.

Further, three types of characteristic clusters that frequently appear in icosahedral quasicrystals are the Mackay, Bergman, and Tsai-type clusters.[70-73] The specific structures are usually described in terms of overlapping clusters of one of these basic types and sometimes by overlapping clusters of two different types. For the comparative review, see, *e.g.*, the monograph by Steurer and Deloudi.[14] On the contrary, we came to conclusion that exactly three different clusters must simultaneously exist in any specific icosahedral structure. Moreover, besides stereochemical restrictions and favorable cluster energetics,[74,75] the icosahedral clusters can have pure geometrical reasons of being compatible with hierarchicity. The same geometrical reasons can cause the appearance of defect clusters like the icosahedron with an omitted vertex – in full accordance with experimental results of Loreto *et al.*,[34] who also mentioned the existence of "invalid" clusters in specific quasicrystalline structures.

Discussion

First of all, we have to emphasize that we didn't introduce any new tilings. The subject of interest is the well-known Socolar-Steinhardt tiling.[3,4] We do have offered a new approach that makes possible to treat the structure of icosahedral quasicrystals without appealing to higher dimensions. This pursuit is far from trivial. We would like to give a quotation from an article by Yamamoto, Takakura and Tsai[58] – "It is clear that in order to describe aperiodic crystal structures such as quasicrystals, the description in a higher-dimensional space is inevitable." So, we started with the assumption that seemed to contradict common sense. As a result, we succeeded to reveal some new aspects of the Socolar-Steinhardt tiling that plays a key role in understanding the special features of icosahedral packings.

There are three kinds of infinite packings with exact icosahedral point symmetry. They represent the only Socolar-Steinhardt tiling and differ by the choice of the origin. The corresponding three types of ideally ordered finite blocks are uniformly distributed within the entire tiling. The further the blocks are from one another, the larger they are. All the three characteristic packings can be generated from single cells or from trivial clusters by using the unique substitution rules. The quasi-unit cells can be easily expanded in all directions producing infinite self-similar rods and layers.

Further, the ideal infinite structure of a single-component icosahedral quasicrystal may be generated from a single atom after the same rules. The positions of all atoms become predetermined after the only atom is placed at the origin.

We hope that we have given enough examples to demonstrate the accuracy of our approach. The main benefit is that we do not need the higher-dimensions since the iterative and recursive substitution algorithm is derived[48] and a specific decoration method is chosen. The main problem is – How to incorporate the fractal approach into the standard fitting procedure, if necessary? The comparison of the experimental and computed diffraction patterns needs a more suitable algorithm to calculate the Fourier transform for the self-similar distribution of point masses rather than the trivial point-by-point counting. The calculation of the *n*D diffraction pattern within the frameworks of high-dimensional crystallography is based on the standard *n*D reciprocal lattice and thus encounters no additional difficulties. On the contrary, the problem of diffraction of self-similar structures is far from solution. We would like to refer the reader to the paper by Lenz[76] to have a look at the list of open problems in the mathematical diffraction theory, concerning especially the aperiodic structures.

How to derive the right decoration method for the quasi-unit cells for a complicated multi-component structure from the experimental diffraction pattern, even though a set of relatively preferred atomic configurations is known? Humbly, we have to admit that the higher-dimensional approach remains still preferable here, at least as far as regarding this specific problem. However, it may be put aside as soon as the cell decoration is finished.

On the other hand, our approach may become an indispensable tool in predicting the structures of artificial solids. We can imagine a substitution packing irrelative of the cluster energetics at all, exactly in the same manner as crystallographers describe the Bravais lattices irrelative of the fact, whether some positions are occupied by atoms or not. Such approach allowed us to derive the simplest structures of single-component icosahedral quasicrystals, as well as to reveal some special features like triads of co-existing characteristic clusters and the essential asymmetry in cell decoration. This seems to have largely escaped the attention of researchers.

Next problem is related to the compatibility with the canonical tiling.[39] We have used the inflation factor of τ^3, whereas the canonical Danzer tiling has the inflation factor of τ. How to decorate the zonohedral tiling by placing additional sites within every zonohedron to obtain the canonical tiling, if

possible? We can put forward a hypothesis that, if both tilings would be deflated infinitely many times, then they both would converge to the common fractal parent. Earlier, we introduced the concept of non-Euclidean parent structures with highest possible symmetry that reveals in various daughter structures as hidden or incomplete.[77]

Icosahedral quasicrystals may be classified into the P, I, and F-types based on the primitive, body-centered, and face-centered unit cells in hyperspace, respectively.[78] How to decorate the quasi-unit cells in zonohedral tiling to obtain three types of quasilattices, if possible?

Next problem is the microscopical interpretation of the phason modes.[79] In the high-dimensional picture of quasicrystals, phason modes are considered as a result of the invariance of the free energy with respect to the cut space. On the contrary, we have shown that ideal quasicrystalline packings may be described without any cut-and-project procedure by usual side-by-side stacking of quasi-unit cells in the ordinary 3D space. Every unit cell is obliged to occupy exactly the predetermined position, be in crystalline or quasicrystalline idealized structure. How to imagine the phason modes when the hyperspace and cutting procedure were not used at all?

The next problem is relating to the possible reduction in subgroup procedure applied to the symmetry group of the fractal parent. Strictly speaking, the most inner tetrahedral shell in the Tsai-cluster may cause the symmetry lowering of the entire structure, accompanied by corresponding rearrangements of atoms in the outer cells. How are we, if possible, to take into account the possible symmetry breaking[80] within the frameworks of fractal approach?

Now we would like to discuss the most complicated and disputable aspects of our work in connection with the fundamental packing problem. Recall that the Hilbert's 18th problem – *Building up of space from congruent polyhedra* – is assumed to be completely resolved. We have shown that the quasi-unit cells may be stacked in three-dimensional space face-to-face without any gaps between them producing the whole infinite icosahedral structure in the same manner as the usual periodic crystals may be generated by multiplication of their unit cells by the symmetry elements of corresponding Fedorov space groups. The only difference is that there are four unit cells instead of one single unit cell for usual periodic crystal. The formal difference disappears, if we refer to the four separated cells as a single non-simply connected fundamental domain. Do quasicrystals represent a part of the 18th problem? Does there exist an opportunity to look at uniform Delaunay sets[81,82] in a new way tacking into account the corrected notion of uniformity?

Further, when the spatial distribution of atoms within the unit cell of the conventional periodic crystal is of particular interest, the opposite sides of the unit parallelepiped are usually considered to be equal. Three cyclic boundary conditions should be set – for every pair of opposite faces. When considering the Socolar-Steinhardt tiling, another three boundary conditions should be set for another three types of faces – F_1, F_2, and F_3. The valid golden rhombohedron that could be used as a unit cell for some conventional periodic crystal must have equivalent opposite faces to comply with translations. In contradistinction, the rhombohedron that could serve as a quasi-unit cell for some aperiodic crystal necessarily must have inequivalent opposite faces. We would like to attract the reader's attention to the discussion between Hargittai and Pauling, who said[83] that "you can always fit something if you pick a large enough lattice parameter." We therefore raise the question whether or not the spatial atomic distribution obtained under cyclic boundary conditions may be immediately transferred onto the aperiodic case? If the difference in boundary conditions is essential, so that fundamentally new packings may appear, then the next question arises: What is the densest icosahedral packing?

Pauling adhered to the opinion that quasicrystals are conventional twins of cubic crystals with very large unit cells.[84] We held the opinion that, in contrast, the quasicrystals may give some new insight into the problem of lattice/quasilattice interfaces. Indeed, compare the five-fold and two-fold layers (Figs. 7 and 9). Both have coinciding vertical chains of polyhedra that correspond to the intersection line between two projection planes (compare with the Fig. 7 in the paper by Steurer[7]). Combine the left part of the five-fold layer with the right part of the two-fold layer into one. This corresponds to the cross-section of the entire three-dimensional structure by a kinked surface. Now leave a three-dimensional imagination behind for a while and consider the tilings as simple plane decorations with multicolored carpet tiles. What do we see? We see a plane tiling combined from two different parts with apparently incompatible symmetry, built of units from a common set of tiles, with no clear boundaries between "five-fold" and "two-fold" regions. Surely, these are not the conventional twins. Earlier, Shevchenko discussed the new kind of interfaces in nanoparticles, which description is beyond the classical crystallographic concepts of twinning and syntactic intergrowth.[85,86] He used the figurative association with a centaur – a half-human and half-horse composition without clearly seen boundaries between incompatible parts and gradual transition from one part to another.

Another question relating to the flat interpretation – Does there exist another five-fold plane tiling besides the famous Penrose tiling? Recall that we have used the inflation factor of τ^3 to derive our colored five-fold carpet.

We would like to quote the work of Senechal:[82] "In the second stage of the quasicrystal revolution, tilings are receding to the background and clusters moving to the foreground. We will still need polyhedra: not to tile space, but to hang the clusters on." So, we still need polyhedra: to tile space, as well as to hold clusters inside – in order to derive infinite atomic structures with ideal icosahedral order, to obtain characteristic clusters compatible with self-similarity, to understand the interlinkage of clusters into the whole structure, and others.

Our results may stimulate further research toward improved understanding of the basic principles underlying the diffraction by aperiodic crystals,[87] as well as open new perspectives in templated quasicrystalline ordering,[88,89] soft matter chemistry,[90,91] and optics of photonic quasicrystals.[92,93]

The derived models may be useful in designing the new structures of icosahedral intermetallic nanoclusters, polyhedral coordination cages, nanocontainers, wheel-shaped nanoclusters, metal-organic frameworks, new mesoporous materials, and others.[94-100]

Conclusions

An accurate tiling approach for the structural description of icosahedral quasicrystals is offered. The iterative and recursive inflation/deflation procedure with subsequent decoration of quasi-unit cells makes it possible to derive the atomic structure of icosahedral quasicrystals.

The possibility is shown to derive the ideal infinite structure of a single-component icosahedral quasicrystal starting with a single atom placed at the origin.

Acknowledgements

I thank Jelena R. Kambak for the proofreading and writing assistance.

Notes and references

1 D. Shechtman, I. Blech, D. Gratias and J.W. Cahn, *Phys. Rev. Lett.*, 1984, **53**, 1951.
2 D. Levine and P.J. Steinhardt, *Phys. Rev. Lett.*, 1984, **53**, 2477.
3 D. Levine and P.J. Steinhardt, *Phys. Rev. B*, 1986, **34**, 596.
4 J.E.S. Socolar and P.J. Steinhardt, *Phys. Rev. B*, 1986, **34**, 617.
5 A.L. Mackay, *Physica A*, 1982, **114**, 609.
6 H. Takakura , C.P. Gómez, A. Yamamoto, M. de Boissieu and A.P. Tsai, *Nature Mater.*, 2007, **6**, 58.
7 W. Steurer, *Chem. Soc. Rev.*, 2012, **41**, 6719.
8 E. Abe, *Chem. Soc. Rev.*, 2012, **41**, 6787.
9 A.P. Tsai, *Chem. Soc. Rev.*, 2013, **42**, 5352.
10 C. Cui, M. Shimoda and A.P. Tsai, *RSC Adv.*, 2014, **4**, 46907.
11 M. de Boissieu, *Struct. Chem.*, 2012, **23**, 965.
12 T. Janssen and A. Janner, *Acta Cryst.*, 2014, **B70**, 617.
13 M. Baake and U. Grimm, *Chem. Soc. Rev.*, 2012, **41**, 6821.
14 W. Steurer and S. Deloudi, *Crystallography of Quasicrystals: Concepts, Methods and Structures*, Springer, Berlin, Heidelberg, 2009.
15 A. Yamamoto and H. Takakura, in *Quasicrystals*, ed. T. Fujiwara and Y. Ishii, Elsevier, Amsterdam, 2008, pp. 11–47.
16 J.M. Dubois, *Chem. Soc. Rev.*, 2012, **41**, 6760.
17 R. Lifshitz, *Found. Phys.*, 2003, **33**, 1703.
18 F. Dyson, *Notices Amer. Math. Soc.*, 2009, **56**, 212.
19 M. Senechal and J.E. Taylor, *Math. Intell.*, 2013, **35**, 1.
20 P. Bak, *Phys. Rev. Lett.*, 1986, **56**, 861.
21 W. Steurer and S. Deloudi, *Acta Cryst.*, 2008, **A64**, 1.
22 P. Kramer and R. Neri, *Acta Cryst.*, 1984, **A40**, 580.
23 E.O. Harriss and J.S.W. Lamb, *Theor. Comput. Sci.*, 2004, **319**, 241.
24 W. Steurer and S. Deloudi, *Struct. Chem.*, 2012, **23**, 1115.
25 R. Strzalka, I. Buganski and J. Wolny, *Acta Cryst.*, 2015, **A71**, 279.
26 C.L. Henley, *Phys. Rev. B*, 1991, **43**, 993.
27 M. Duneau and D. Gratias, in *Coverings of Discrete Quasiperiodic Sets: Theory and Applications to Quasicrystals*, ed. P. Kramer and Z. Papadopolos, Springer Tracts in Modern Physics, vol. **180**, Springer, Berlin, 2003, pp. 23–62.
28 A.P. Tsai, *Sci. Technol. Adv. Mater.*, 2008, **9**, 013008.
29 P. Guyot and M. Audier, *C. R. Phys.*, 2014, **15**, 12.
30 E. Abe, Y. Yan and S.J.R. Pennycook, *Nature Mater.*, 2004, **3**, 759.
31 A.I. Goldman and R.F. Kelton, *Rev. Mod. Phys.*, 1993, **65**, 213.
32 C.P. Gómez and S. Lidin, *Phys. Rev. B*, 2003, **68**, 024203.
33 V.E. Dmitrienko and V.A. Chizhikov, *Crystallogr. Rep.*, 2006, **51**, 552.
34 L. Loreto, R. Farinato, S. Catallo, C. Janot, G. Gerbasi and G. De Angelis, *Physica B*, 2003, **328**, 193.
35 F. Puyraimond, M. Quiquandon, D. Gratias, M. Tillard, C. Belin, A. Quivy and Y. Calvayrac, *Acta Cryst.*, 2002, **A58**, 391.
36 G. Gebresenbut, M.S. Andersson, P. Beran, P. Manuel, P. Nordblad, M. Sahlberg and C.P. Gómez, *J. Phys. Condens. Matter.*, 2014, **26**, 322202.
37 Q. Lin and J.D. Corbett, *J. Am. Chem. Soc.*, 2006, **128**, 13268.
38 P.J. Steinhardt, H.C. Jeong, K. Saitoh, M. Tanaka, E. Abe and A.P. Tsai, *Nature*, 1998, **396**, 55.
39 L. Danzer, *Discr. Math.*, 1989, **76**, 1.
40 M. Mihalkovič, W.J. Zhu, C.L. Henley and M. Oxborrow, *Phys. Rev. B*, 1996, **53**, 9002.
41 M. Mihalkovič and M. Widom, *Phil. Mag.*, 2006, **86**, 519.
42 L. Danzer, Z. Papadopolos and A. Talis, *Int. J. Mod. Phys. B*, 1993, **7**, 1379.
43 F. Gähler, *J. Non-Cryst. Solids*, 1993, **153-154**, 160.
44 M. Quiquandon, R. Portier and D. Gratias, *Acta Cryst. A*, 2014, **A70**, 229.
45 N. Fujita, H. Takano, A. Yamamoto and A.P. Tsai, *Acta Cryst. A*, 2013, **A69**, 322.
46 M. Engel, P.F. Damasceno, C.L. Phillips and S.C. Glotzer, *Nature Mater.*, 2015, **14**, 109.
47 M. de Boissieu, *Nature Mater.*, 2015, **14**, 18.
48 A.E. Madison, *RSC Adv.*, 2015, **5**, 5745.
49 C. Bandt and P. Gummelt, *Aequ. Math.*, 1997, **53**, 295.
50 A.E. Madison, *Phys. Solid State*, 2013, **55**, 855.
51 A.E. Madison, *Phys. Solid State*, 2014, **56**, 1706.
52 A.E. Madison, *Struct. Chem.*, 2015, **26**, 923.
53 N.P. Frank, *Expo. Math.*, 2008, **26**, 295.
54 W.P. Thurston, *Groups, Tilings, and Finite State Automata*, AMS Colloquium Lecture Notes, Amer. Math. Soc., Boulder, 1989.
55 C. Radin, *Ann. Math.*, 1994, **139**, 661.
56 C. Goodman-Strauss, *Ann. Math.*, 1998, **147**, 181.
57 N.P. Frank and M.F. Whittaker, *Math. Intell.*, 2011, **33**, 7.
58 A. Yamamoto, H. Takakura and A.P. Tsai, *Phys. Rev. B*, 2003, **68**, 094201.
59 H.R. Sharma, M. Shimoda and A.P. Tsai, *Adv. Phys.*, 2007, **56**, 403.
60 P. A. Thiel, *Ann. Rev. Phys. Chem.*, 2008, **59**, 129.
61 R. McGrath, J.A. Smerdon, H.R. Sharma, W. Theis and J. Ledieu, *J. Phys. Condens. Matter*, 2010, **22**, 084022.
62 M. Gierer, M.A. Van Hove, A.I. Goldman, Z. Shen, S.L. Chang, P.J. Pinhero, C.J. Jenks, J.W. Anderegg, C.M. Zhang and P. A. Thiel, *Phys. Rev. B*, 1998, **57**, 7628.
63 B. Ünal, C.J. Jenks and P.A. Thiel, *J. Phys. Condens. Matter.*, 2009, **21**, 055009.
64 H.R. Sharma, M. Shimoda, K. Sagisaka, H. Takakura, J.A. Smerdon, P.J. Nugent, R. McGrath, D. Fujita, S. Ohhashi and A.P. Tsai, *Phys. Rev. B*, 2009, **80**, 121401.
65 Krajčí and J. Hafner, *Phys. Rev. B*, 2005, **71**, 054202.
66 G. Kasner and Z. Papadopolos, *Phil. Mag.*, 2006, **86**, 813.
67 C. Cui, P.J. Nugent, M. Shimoda, J. Ledieu, V. Fournée, A.P. Tsai, R. McGrath and H.R. Sharma, *J. Phys. Condens. Matter.*, 2012, **24**, 445011.
68 C. Cui, P.J. Nugent, M. Shimoda, J. Ledieu, V. Fournée, A.P. Tsai, R. McGrath and H.R. Sharma, *J. Phys. Condens. Matter*, 2014, **26**, 015001.
69 P. Thiel, *Nature Mater.*, 2007, **14**, 18.
70 A.L. Mackay, *Acta Crystallogr.*, 1962, **15**, 916.
71 G. Bergman, J.L.T. Waugh and L. Pauling, *Acta Crystallogr.*, 1957, **10**, 254.
72 A.P. Tsai, J.Q. Guo, E. Abe, H. Takakura and T.J. Sato, *Nature*, 2000, **408**, 537.
73 K.H. Kuo, *Struct. Chem.*, 2002, **13**, 221.
74 V.M. Berns and D.C. Fredrickson, *Inorg. Chem.*, 2013, **52**, 12875.
75 Y. Guo, T.E. Stacey and D.C. Fredrickson, *Inorg. Chem.*, 2014, **53**, 5280.
76 D. Lenz, *Phil. Mag.*, 2008, **88**, 2059.
77 V.Ya. Shevchenko, A.E. Madison and A.L. Mackay, *Acta Crystallogr.*, 2007, **A63**, 172.
78 D.A. Rabson, N.D. Mermin, D.S. Rokhsar and D.C. Wright, *Rev. Mod. Phys.*, 1991, **63**, 699.
79 M. de Boissieu, *Chem. Soc. Rev.*, 2012, **41**, 6778.
80 R. Lifshitz, *Isr. J. Chem.*, 2011, **51**, 1156.
81 N.P. Dolbilin, H. Edelsbrunner and O.R. Musin, *Russ. Math. Surv.*,

2012, **67**, 781.
82 M. Senechal, *Proc. Steklov Inst. Math.*, 2015, **288**, 259.
83 I. Hargittai, *Isr. J. Chem.*, 2011, **51**, 1144.
84 L. Pauling, *Nature*, 1985, **317**, 512.
85 V.Ya. Shevchenko, A.E. Madison and V.B. Glushkova, *Glass Phys. Chem.*, 2001, **27**, 400.
86 V.Ya. Shevchenko, M.I. Samoilovich, A.L. Talis and A.E. Madison, *Glass Phys. Chem.*, 2005, **31**, 407.
87 J.G. Escudero and J.G. Garcia, *Mod. Phys. Lett. B*, 2003, **17**, 303.
88 R. McGrath, J. Ledieu, E.J. Cox and R.D. Diehl, *J. Phys. Condens. Matter.*, 2002, **14**, R119.
89 J.A. Smerdon, K.M. Young, M. Lowe, S.S. Hars, T.P. Yadav, D. Hesp, V.R. Dhanak, A.P. Tsai, H.R. Sharma and R. McGrath, *Nano Lett.*, 2014, **14**, 1184.
90 T. Dotera, *Isr. J. Chem.*, 2011, **51**, 1197.
91 S.C. Glotzer and M. Engel, *Nature*, 2011, **471**, 309.
92 K. Edagawa, *Sci. Technol. Adv. Mater.*, 2014, **15**, 034805.
93 A.N. Poddubny and E.L. Ivchenko, *Physica E*, 2010, **42**, 1871.
94 S. Alvarez, *Dalton Trans.*, 2005, 2209.
95 A.A. Pankova, T.G. Akhmetshina, V.A. Blatov and D.M. Proserpio, *Inorg. Chem.*, 2015, **54**, 6616.
96 W. Cullen, S. Turega, C.A. Hunter and M.D. Ward, *Chem. Sci.*, 2015, **6**, 625.
97 A. Müller and P. Gouzerh, *Chem. Eur. J.*, 2014, **20**, 4862.
98 U. Kortz, A. Müller, J. van Slageren, J. Schnack, N.S. Dalal, M. Dressel, *Coord. Chem. Rev.*, 2009, **253**, 2315.
99 I. Nakamura, H.N. Miras, A. Fujiwara, M. Fujibayashi, Y.F. Song, L. Cronin and R. Tsunashima, *J. Am. Chem. Soc.*, 2015, **137**, 6524.
100 M. O'Keeffe, *APL Mat.*, 2014, **2**, 124106.